Articles

Controlled Synthesis of Photochromic Polymer Brushes by Atom Transfer Radical Polymerization

Martin Piech and Nelson S. Bell*

Sandia National Laboratories, P.O. Box 5800-1411, Albuquerque, New Mexico 87185

Received June 17, 2005; Revised Manuscript Received December 9, 2005

ABSTRACT: This work reports on the grafting of methyl methacrylate polymer brushes containing spirobenzopyran pendant groups from flat silica surfaces and colloidal particles utilizing atom transfer radical polymerization (ATRP). The reaction conditions were optimized with respect to the kind of surface bound initiator, the type of halide and ligand used in the catalytic complex, the presence/absence of untethered initiator, and solvent type. This enabled synthesis of coatings up to 80 ± 3 nm thick with controlled spirobenzopyran content. While polymerization kinetics indicate the presence of chain termination reactions, the "living" character of the process is confirmed by controlled formation of block copolymer brushes. UV/vis spectroscopy was used to characterize the UV-induced isomerization of spirobenzopyran to zwitterionic merocyanine and the thermal back-reaction. Spectral and kinetic analyses of this latter bleaching process points to the existence of free and associated merocyanines in the polymeric brush in both tetrahydrofuran and toluene. However, stabilization of merocyanine species by the polymer matrix is considerably greater in toluene with thermal back-reaction rates approaching those determined for solid dry films.

Introduction

The ability to reversibly alter system properties through application of remote stimuli such as light is highly attractive in a number of technologically relevant fields. Specifically, the optical actuation of nanointeractions to impact behavior on both the nano- and microscales has potential applications in directed nanostructure formation, microfluidic rheology, and tribological control. Photochromic compounds with reversible, specific wavelength-induced changes in molecular properties have been incorporated into various material systems including surface bound monolayers,[1−5] Langmuir monolayers,[6,7] Langmuir−Blodgett films,[1−6] polymeric brushes,[8,9] photocontrollable surfactants,[10,11] liquid crystalline materials,[4,12,13] polymeric matrices,[14−25] organic/inorganic hybrid systems,[26,27] and colloidal particles.[28−31] This has led to reversible changes in system properties such as conductivity,[2,16] wetting behavior,[3,5] adsorption,[15,25,29] metal ion complexation,[20,32] chiral expression,[14,33] surface morphology,[1,6,21] gelation,[23,34] solution viscosity,[19,22] association/solubility,[10,18,20,25] mechanical effects,[17,24] colloidal system stability,[28,31] and membrane permeability.[8,9] Apart from applications in the area of optical memory and optical recording, these developments offer opportunities for designing sensor materials, actuators, and other photomodulated devices.

Despite recent advances in the area of photoactive material synthesis, the formation of robust, well-defined surface coatings with greater than monolayer coverage of photochromic moieties would be a welcome addition. Here, we describe a general process of controllably grafting polymeric matrixes containing photochromic molecules from surfaces using a "living" polymerization approach. Particularly, spirobenzopyran/methyl methacrylate (pSP-*co*-MMA) copolymers were grafted from flat silica surfaces and colloidal particles utilizing atom transfer radical polymerization (ATRP).

Experimental Section

Materials. Methyl methacrylate (Aldrich, 99%) was freed of inhibitor by passing through a MEHQ removing column (Aldrich, cat. no. 306312). Similarly, styrene (Acros, SP) was passed through a *tert*-butylcatechol removing column (Aldrich, cat. no. 306320). The monomers were then distilled under reduced pressure. All solvents were at least HPLC grade and used without further purification. Similarly, CuBr (Aldrich, 99.999%), CuCl (Aldrich, 99.999%), $CuBr_2$ (Aldrich, 99.99%), $CuCl_2$ (Aldrich, 99+%), PMDETA (Aldrich, 99%), Me_4Cyclam (Aldrich, 98%), and other reagents were used as received. Tris[2-(dimethylamino)ethyl]amine (TREN) ligand was prepared by a known literature procedure.[35] All liquid reagents used in polymerization reactions were degassed using three freeze−pump−thaw cycles and then transferred into a dry, O_2-free glovebox. Spherical, monodisperse, silica particles (Fuso Chemical Co., Ltd., grade SP-03B and SP-1B) were received as dry powders and used without further purification. Substrates employed were either 1 in.^{2} fused silica coverslips (0.0197 ± 0.002 in. thick; Valley Design) or test type n-doped silicon (100) wafers with 19.7−27.6 Å thick oxide layer (Allied Bendix) cut into 1 in.^{2} pieces.

Initiator Synthesis. Undecen-1-yl-2-bromo-2-methylpropionate and (11-(2-bromo-2-methyl)priopionyloxy)undecyltrichlorosilane were synthesized according to a published procedure.[36] In the case of undecen-1-yl 2-chloropropionate and (11-(2-chloro)priopionyloxy)undecyltrichlorosilane an analogous protocol was adopted.

Monolayer Self-Assembly. A procedure similar to that reported by Matyjaszewski et al. was followed for attachment of initiator to fused silica coverslips and silicon (100) wafers.[36] In the case of silica colloids, this was modified slightly. Specifically, the particles

10.1021/ma0512760 CCC: $33.50
Published on Web 01/13/2006

(20 g) were added to 50 mL of anhydrous toluene in a drybox. The suspension was sonicated for 5 min and shaken to break apart larger aggregates. Trichlorosilane (see above) was then added to give a 155 mM solution in the case of 284 nm diameter particles and a 65 mM solution for the 927 nm diameter spheres. These concentrations were chosen to provide at least 5 times the excess of monolayer coverage. Following overnight reaction at 65 °C under stirring, the particles were washed by centrifugation/decantation cycles with anhydrous toluene (2 cycles), tetrahydrofuran (THF; 2 cycles), and methylene chloride (CH_2Cl_2; 2 cycles). After washing, the treated colloids were dried under vacuum, sealed in a dark container, and stored in the drybox until use.

Spirobenzopyran Monomer Synthesis. 1′-(2-Hydroxyethyl)-3′,3′-dimethyl-6-nitrospiro(2*H*-1-benzopyran-2,2′-indoline) (SP alcohol) was prepared according to a published protocol.[37] While synthesis of 1′-(2-methacryloxyethyl)-3′,3′-dimethyl-6-nitrospiro-(2*H*-1-benzopyran-2,2′-indoline) (SP) has been reported elsewhere,[38] a different method was adopted here. Specifically, a solution of SP alcohol (15.0 g, 42.6 mmol) and triphenylphosphine (20.1 g, 76.7 mmol) in THF (640 mL) was cooled to 0 °C under Ar. Diethylazodicarboxylate (13.2 g, 75.8 mmol) was then added, and the mixture was stirred for 10 min. Following the addition of methacrylic acid (6.6 g, 75.8 mmol) and after removal of cooling, the solution was stirred for 24 h at room temperature. The solvent was dried using a rotary evaporator and the product passed through the silica gel column to remove oxyphosphonium salts. The crude product (21.9 g) was recrystallized from hexanes to give 14.8 g (35.1 mmol) of pale green crystals in 82.5% yield. ^{1}H NMR (500 MHz $CDCl_3$) δ: 1.17 (s, 3H); 1.28 (s, 3H); 1.92 (s, 3H); 3.38−3.63 (m, 2H); 4.3 (t, 2H); 5.56 and 6.07 (d, 2H); 5.87 (d, 1H); 6.73 (q, 2H); 6.89 (q, 2H); 7.09 (d, 1H); 7.17−7.28 (m, 1H); 7.96−8.05 ppm (m, 2H).

General Polymerization Procedures. The reactions were carried out in a moisture- and O_2-free glovebox under different conditions. Specifically, monomer concentration, SP/MMA monomer ratio, types of initiator surfaces, copper halide catalysts, coordinating ligands, and solvents were all varied. The polymerizations were performed in glass jars with sealable tops or in round-bottom flasks equipped with septa when it was necessary to remove samples during the reaction. Representative synthesis of poly(SP-*co*-MMA) brush layers containing 20 mol % SP ($pSP_{0.2}$-*co*-$MMA_{0.8}$ for short) was as follows: Contents of a glass jar filled with SP (16.0 g, 38.0 mmol), MMA (15.2 g, 152 mmol), and THF (4 mL) were stirred until SP monomer dissolved completely. To this a catalyst solution comprised of CuBr (163 mg, 0.73 mmol), $CuCl_2$ (4.86 mg, 0.035 mmol), PMDETA (0.90 mL, 4.31 mmol), and THF (0.37 mL) was added, and the mixture was stirred for 1−2 min. Following the removal of stirring, a custom holder containing 5−10 silica substrates modified with an initiator SAM was submerged in this monomer/catalyst mixture. After sealing tightly with a screw-top lid, the container was placed in a thermostated oil bath kept at 65 °C, and the reaction was allowed to proceed for 6−24 h. Upon removal from the solution, samples were immediately transferred into anhydrous THF and cleaned under ultrasound for 15 min. This cleaning procedure was repeated in dry toluene and then again in CH_2Cl_2. The samples were kept under anhydrous toluene in a glovebox when not in use.

When colloidal particles were treated, this procedure had to be adopted slightly. In the glovebox, dry particles modified with initiator SAMs were first dispersed into a chosen solvent by 1 min sonication in an ultrasonic bath. This suspension was then transferred into a stirred monomer/catalyst solution via a syringe. Upon reaction completion, the mixture was removed from the glovebox, and the particles were washed by a centrifugation/decantation sequence using anhydrous THF (5 cycles) and anhydrous toluene (5 cycles) or until the supernatant was free of SP monomer. The colloids were then stored as toluene suspensions in sealed, dark bottles within a separate drybox.

Polymerizations with a Free Initiator. To facilitate polymer synthesis in the bulk, a sacrificial initiator (i.e., ethyl 2-chloropropionate or ethyl 2-bromoisobutyrate) was added to the polymerization mixture at the reaction onset. Following the synthesis and removal of modified silica surfaces or particles, the free polymer was recovered by (re)precipitation twice in methanol.

Polymerizations from pSP-*co*-MMA Brushes. In the first step, pSP-*co*-MMA brushes on silica colloids were prepared as described above, except for quenching the reaction with excess $CuBr_2$ before it reached completion. The particles were then cleaned centrifugation/decantation sequence in the usual manner before being dried and reintroduced into the glovebox. The second polymerization step was conducted with either an identical SP/MMA mixture or utilizing styrene monomer. In the latter case, the particles (0.072 g) were first dispersed in anisole (0.5 mL) using ultrasound energy to break apart aggregates. Next, CuBr (9.9 mg, 0.044 mmol), $CuCl_2$ (0.18 mg, 0.0013 mmol), PMDETA (29 mg, 0.17 mmol), and styrene (1.36 g, 13 mmol) were added. The polymerization was allowed to proceed in a sealed flask for 20 h at 95 °C under stirring. The solidified reaction mixture was then removed from the glovebox and dissolved in THF. The particles were washed by a centrifugation/decantation sequence using anhydrous THF (5 cycles) and anhydrous toluene (5 cycles).

Scanning Electron Microscopy. Hitachi S4500 field emission SEM operating at 5 kV was used to image particles deposited onto freshly cleaved mica and sputter coated with Au/Pd (coating thickness ~8 nm). Sizes of the core silica particles were determined from SEM micrographs that show well-packed monolayer films utilizing IMIX particle analysis software (Princeton Gamma Tech). On the basis of the analysis of at least 900 particles, the diameters of SP03B and SP1B silica spheres were determined to be 283 ± 11 and 927 ± 24 nm, respectively.

Transmission Electron Microscopy. A Philips CM30 TEM/STEM operating at 300 kV was employed to image polymer brushes grafted onto the silica core particles. The polymer layer thickness was estimated from 8 to 20 separate measurements per sample.

Particle Density Determination. The density of polymer-coated particles was calculated from the known core and shell sizes using 2.1 g/cm^3 as the density of silica core (value provided by the manufacturer) and 1.191 ± 0.012 g/cm^3 for the density of $pSP_{0.2}$-*co*-$MMA_{0.8}$ copolymer brush. This latter value was obtained by determining the density of free $pSP_{0.2}$-*co*-$MMA_{0.8}$ copolymer.

^{1}H Solution NMR Spectroscopy. Solution ^{1}H NMR analyses were performed on a Bruker DRX400 spectrometer and were referenced against residual solvent peaks or external TMS. Samples were prepared by dispersing 50−250 mg of polymer-modified colloids or 5−15 mg of free polymer into 1 g of 99.998% CD_2Cl_2. The SP content of pSP-*co*-MMA copolymer brushes and free copolymers was obtained by comparing integrated peak areas in the range $5.37 < \delta < 9$ ppm (corresponding to 9 SP protons) to the peak areas in the range $0 < \delta < 5.27$ ppm (corresponding to 15 SP and 8 MMA protons).

Gel Premeation Chromatography. GPC measurements were carried out on a Polymer Laboratories Inc. PL-GPC210 system with incorporated differential refractometer detector operating at 40 °C. The HPLC-grade THF was used as the mobile phase at a flow rate of 1.0 mL/min. The GPC system was equipped with two in-series PLgel 5μm MIXED-C columns to cover an exclusion limit of 200−2 000 000. The instrument was calibrated with five different linear low polydispersity (i.e., $M_w/M_n < 1.11$) polystyrene standards having molecular weights $M_w = 4920-1\,065\,000$ (symbols M_n and M_w represent number- and weight-averaged molecular weight, respectively).

UV−vis Spectroscopy. UV−vis absorption spectra of monomer, polymer, and modified particles in THF and toluene were recorded with an Ocean Optics USB2000 spectrometer coupled to a pulsed xenon lamp (Model PX-2, Ocean Optics). A custom-made cell holder allowed simultaneous recording of absorption and lateral illumination of the sample with $\lambda = 365 \pm 10$ nm light from a 200 W mercury arc lamp (Oriel) fitted with a band-pass filter. The kinetic rates of SP → MC were determined by monitoring changes in absorbance at the visible absorption maximum during the UV irradiation. Analogously, the MC → SP isomerization kinetics were recorded immediately after the UV treatment.

Table 1. Conditions of Different Polymerization Reactions Used To Synthesize the pSP-*co*-MMA Polymer Brushes on Silica Colloids; Reaction Temperature and Duration Were 65 °C and 18−24 h, Respectively, with All Syntheses Performed in Tetrahydrofuran

expt no.	[mono][a] (mol/L)	SP % rnx[b]	init[c]	CuX,[d] X =	CuY_2,[e] Y =	[ligand][f] (mol/L)	h[g] (nm)
varying reaction control (no. 1, addition of Cu^{II}; no. 2, addition of sacrificial initiator)							
1[h]	3.4	20	Br	Br	Br	2.7×10^{-2}	25.5 ± 1.2
2[h]	3.4	20	Br	Br		2.7×10^{-2}	29.4 ± 4.3
varying initiator type and halogen in the catalytic system							
3	3.8	20	Br	Br	Br	8.6×10^{-2}	24.9 ± 2.6
4	3.8	20	Br	Cl	Cl	7.8×10^{-2}	34.2 ± 3.3
5[i]	3.8	20	Br	Br	Cl	7.8×10^{-2}	49.3 ± 2.2
6	3.8	20	Cl	Cl	Br	7.8×10^{-2}	50.3 ± 1.7
7	3.8	20	Cl	Br	Br	7.8×10^{-2}	55.5 ± 2.3
8	3.8	20	Cl	Cl	Cl	7.8×10^{-2}	57.8 ± 1.3
9	3.8	20	Cl	Br	Cl	7.8×10^{-2}	75.8 ± 2.6
varying ligand type (no. 10 = Me_6TREN, no. 11 = Me_4cyclam, no. 12 = PMDETA)[f]							
10	3.8	20	Cl	Br	Cl	3.2×10^{-2}	32.7 ± 1.7
11	3.8	20	Cl	Br	Cl	3.2×10^{-2}	73.8 ± 6.0
12	3.8	20	Cl	Br	Cl	3.2×10^{-2}	79.5 ± 2.6

[a] Total monomer concentration, [SP] + [MMA]. [b] Content of SP in the reaction mixture expressed as mole percent. [c] Type and concentration of initiator monolayer chemisorbed onto the silica partilces: "Br" stands for (11-(2-bromo-2-methyl)priopionyloxy)undecyltrichlorosilane, while "Cl" denotes (11-(2-chloro)priopionyloxy)undecyltrichlorosilane. Except for experiments 1 and 2, SP1B-type colloidal silica was employed. [d] CuBr (X = Br) or CuCl (X = Cl) was used as catalyst at a concentration of 1.5×10^{-2} to 2.1×10^{-2} mol/L. [e] $CuBr_2$ (Y = Br) or $CuCl_2$ (Y = Cl) was used as the inhibitor at a concentration of 4.9×10^{-4} to 6.4×10^{-4} mol/L, except for experiment 2 where sacrificial initiator was employed to control the reaction. [f] Ligand concentration. In most cases, *N*,*N*,*N*′,*N*″,*N*″-pentamethyldiethylenetriamine (PMDETA) was used, except for experiments 10 and 11, employing tris[2-(dimethylamino)ethyl]amine (Me_6TREN) and 1,4,8,11-tetraaza-1,4,8,11-tetramethylcyclotetradecane (Me_4cyclam), respectively. [g] Polymer brush layer thickness determined from TEM analysis. [h] SP03B type colloidal silica was used in both experiments 1 and 2. In the case of experiment 2, sacrificial initiator, ethyl 2-bromoisobutyrate was added at the reaction onset at a concentration of 2.3×10^{-3} mol/L. [i] In addition to $CuCl_2$ deactivator, free sacrificial initiator, ethyl 2-bromoisobutyrate, was added at the reaction onset at a concentration of 1.9×10^{-3} mol/L.

Scheme 1. Formation of Grafted Polymer Layers

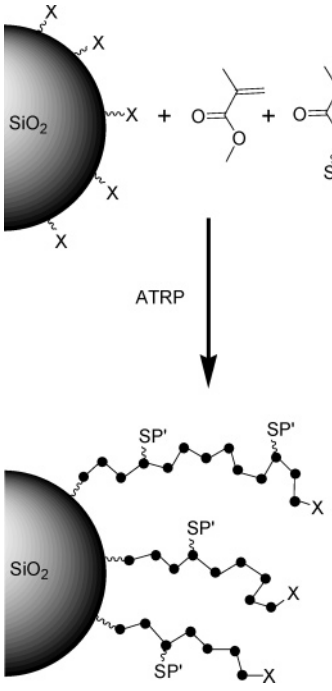

Results and Discussion

Synthesis of Grafted pSP-*co*-MMA Copolymer Brushes. Several polymerization reactions were performed under different conditions in an attempt to identify main control variables and optimize the polymer brush thickness. The results of these experiments along with specific reaction conditions are summarized in Table 1, while the formation of grafted polymer layers via ATRP is illustrated in Scheme 1. A common feature of all syntheses was the use of cuprous halide catalyst and cupric halide deactivator. Together with a suitable ligand, this catalytic system has been well researched in the past and applied to the polymerization of various acrylate and methacrylate monomers.[39−41] Since the initiator concentration on the surface of colloidal particles was very low, addition of the cupric halide deactivator was essential to ensure a controlled polymerization process.[36] In a few cases, sacrificial initiator (i.e., ethyl 2-bromoisobutyrate and ethyl 2-chloropropionate at a concentration of $(2-10) \times 10^{-3}$ M) was utilized instead,[42] generating free pSP-*co*-MMA copolymers in solution along with the grafted brushes. Although both of these approaches produced polymer films of comparable thickness (see experiments 1 and 2 in Table 1), the addition of sacrificial initiator resulted in gelation and complicated further processing.

It is apparent from Table 1 that the choice of the surface bound initiator, Cu^I halide catalyst, and Cu^{II} halide deactivator greatly affects the brush layer thickness (see experiments 3−9). Thus, the use of 2-chloropriopionate instead of 2-bromoisobutyrate initiator groups attached to colloidal particles yielded significantly thicker polymer shells under identical reaction conditions. Similarly, solution polymerization with ethyl 2-chloroisobutyrate vs ethyl 2-bromoisobutyrate offered higher molecular weight pSP-*co*-MMA copolymers characterized by a lower polydispersity index.

Thus, in the case of ethyl 2-choropropionate, $M_n = 78\,310$ g/mol and $M_w/M_n = 1.82$. Meanwhile, $M_n = 45\,270$ g/mol and $M_w/M_n = 2.42$ was obtained with the ethyl 2-bromoisobutyrate reaction. These results are somewhat unexpected, as α-halopropionates are generally less suitable for MMA polymerization due to the low reactivity of their C−X bonds compared with that of the dormant methacrylate terminal.[43] Conversely, more reactive 2-bromoisobutyrate is a unimer model of poly(methacrylate) with a dormant C−Br terminal and has been employed as a versatile initiator for methacrylates, acrylates, and styrenes.[44] However, once formed, the more stable 1-bromoisobutyrate radical reacts more slowly with monomers, giving an increasing chance of recombination with another initiator radical. This is especially likely to occur in dense monolayers on surfaces, as is the case here.

Experiments 3−9 in Table 1 also show that the combination of CuBr catalyst and $CuCl_2$ deactivator affords the thickest polymer brushes for a given initiator choice. This might be caused by the higher reactivity of CuBr toward the initiator

terminal compared to CuCl. Thus, a greater percentage of initiator molecules become activated when CuBr is used as the catalyst. Since the kinetics of brush growth are directly proportional to the number of growing chains, thicker polymer layers are obtained. Analogously, $CuCl_2$ compared to $CuBr_2$ affords slower deactivation of the growing chain ends to their dormant state. This allows a greater number of monomer units to be inserted per activation/deactivation cycle and will yield faster brush growth. However, these are speculative arguments, and detailed mechanistic study would be helpful in answering why the combination of 2-choropropionate initiator, CuBr catalyst, and $CuCl_2$ deactivator affords thickest polymer layers.

Finally, data in Table 1 show that out of the three ligands examined here PMDETA provided thickest pSP-*co*-MMA brushes (compare experiments 10−12 in Table 1). This might result from PMDETA having the highest solubility in the monomer/solvent mixture.

Several different solvents (e.g., benzene, toluene, anisole, tetrahydrofuran, and *N*,*N*-dimethylformamide) produced similar synthesis results. However, THF became the solvent of choice due to its excellent pSP-*co*-MMA copolymer solubility and low viscosity. It should be mentioned that presence of moisture in the reaction mixture significantly retarded copolymer film growth (i.e., 3×10^{-3} mol/L of water reduced the final brush thickness by ~60%). This effect can be attributed to lowered SP solubility and its conversion into the bulkier, more polar MC isomer (see Scheme 2).

Scheme 2. Photoswitching of SP

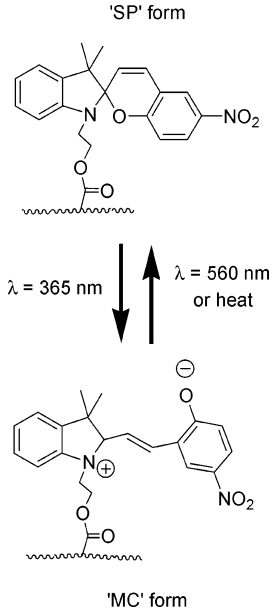

Synthesis of brushes with a general SP/MMA ratio required only that the same monomer proportions are present in the initial reaction mixture. This is illustrated in Figure 1, where the SP content in the copolymer brush mirrors the reaction mixture composition with an error of up to 20%. Similar results were reported for free pSP-*co*-MMA copolymers synthesized via a conventional 2,2′-azobis(isobutyronitrile) (AIBN)-initiated radical polymerization process.[8] Despite the ability to fabricate copolymer films with an arbitrary composition, $pSP_{0.2}$-*co*-$MMA_{0.8}$ brushes (i.e., pSP-*co*-MMA polymer containing 20% mol SP) were synthesized predominantly. The copolymers with this particular composition were shown to undergo a reversible solubility change in toluene upon alternating UV/vis light irradiation.[8] Consequently, when grafted onto colloidal particles,

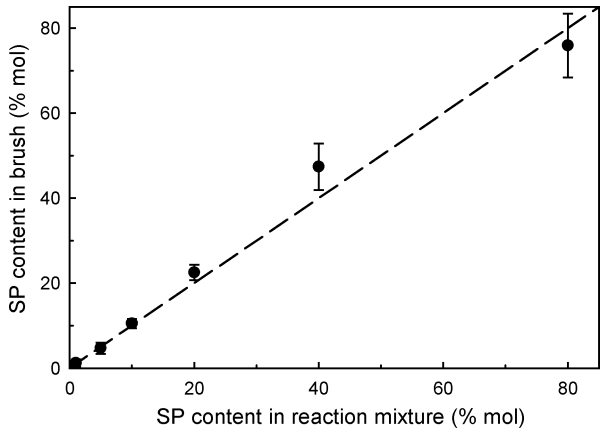

Figure 1. Content of SP molecules in the polymeric brush as a function of reaction mixture composition. The brush was grown from 927 nm diameter SiO_2 colloids modified with (11-(2-chloro)propionyloxy)-undecyltrichlorosilane. Reaction conditions were as follows: [monomer] = 1.2 M, [CuBr] = 1.5×10^{-2} M; [$CuCl_2$] = 6×10^{-4} M; [PMDETA] = 7.7×10^{-2} M in THF solvent with temperature = 65 °C. ^{1}H solution NMR analysis was used to determine the mole percent (mol %) of SP in the polymer brush. The broken line represents azeotropic polymerization.

these copolymer films were especially well suited for study of photocontrolled aggregation and sedimentation phenomena.[45]

The polymer layer thickness and molecular weight data for free polymers synthesized under the same conditions may be combined to estimate a cross-sectional area per chain in the brush, A_{ch}.

$$A_{ch} = \frac{M_n}{h\rho_p N_A} \quad (1)$$

Here, h is the brush thickness, ρ_p is the polymer density, and N_A represents Avogadro's constant. Equation 1 is based on the assumption that surface polymerization and its solution analogue result in polymers with the same molecular weight. This has been shown to be true for a variety of ATRP syntheses.[46−48] In the case of $pSP_{0.2}$-*co*-$MMA_{0.8}$ brushes on silica, $A_{ch} = 2.85 \pm 0.7$ nm^2 was found, which is similar to the value determined for acrylamide brushes prepared via surface-initiated ATRP (i.e., $A_{ch} = 2.8$ nm^2).[41] Given that the cross-sectional area per 2-bromoisobutyrate group is 1.4 nm^2, only 50% of available initiator molecules participated in the polymerization, most likely due to early radical recombination reactions.[49] Reaction kinetics illustrated in Figure 2 for the growth of $pSP_{0.2}$-*co*-$MMA_{0.8}$ brushes from SP1B silica colloids also imply significant loss of active chain ends during the polymerization. Specifically, the plot of layer thickness vs time is nonlinear, while linear relationship is expected in the absence of chain termination.[50] Furthermore, the kinetic data can be well described using models of layer growth that take into account radical combination reactions.[41,51] For example, a simple model of Kim et al. expressed by eq 2 fits Figure 2 data with an R^2 statistic of 0.998.[51]

$$h(t) = (k_2/k_1)\ln(1 + k_1[X]_0 t) \quad (2)$$

Here, $[X]_0$ denotes the starting concentration of active initiator sites, while k_1 and k_2 are the rate constants for radical combination and chain propagation reactions, respectively. Similarly, using a more elaborative model of Xiao et al. to fit the kinetic data gives R^2 value of 0.995.[41] Despite the presence of these termination reactions, pSP-*co*-MMA brushes up to ~80 nm thick could be synthesized in a controllable manner.

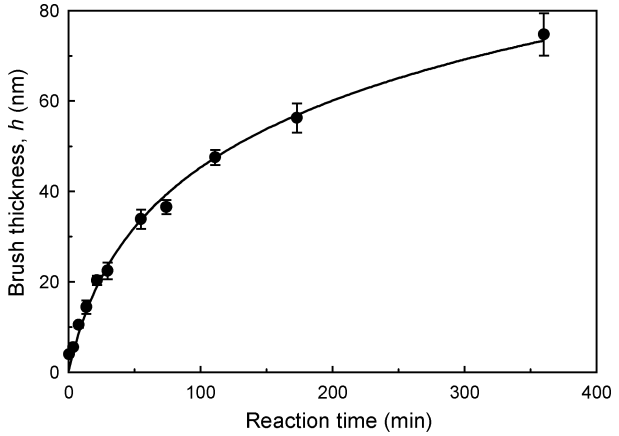

Figure 2. Thickness of $pSP_{0.2}$-*co*-$MMA_{0.8}$ brush vs time. The copolymer film was grown from 927 nm diameter SiO_2 colloids modified with 2-chloropriopionate initiator groups. Polymerization conditions were as follows: [monomer] = 3.3 M, [CuBr] = 1.3×10^{-2} M; [$CuCl_2$] = 6×10^{-4} M; [PMDETA] = 7.5×10^{-2} M in THF solvent with temperature = 65 °C. The line represents fit to eq 2.

Formation of Block Copolymer Brushes. By quenching polymerization before completion with excess deactivator, it was possible to preserve dormant chain ends and allow subsequent block copolymerization. For example, stopping $pSP_{0.2}$-*co*-$MMA_{0.8}$ layer growth from SP1B silica colloids after 74 min gave $h = 36.5 \pm 1.6$ nm (see Figure 2). Following washing, subsequent polymerization from these modified particles under identical reaction conditions (see Figure 2 caption for details) increased the film thickness to 61.1 ± 1.7 nm. Similarly, ATRP of styrene from quenched $pSP_{0.2}$-*co*-$MMA_{0.8}$ brushes with initial layer thickness of 56.3 ± 3.2 nm yielded significantly thicker films characterized by $h = 77.4 \pm 4.5$ nm (see Figure 3). Moreover, the particles modified with these pSP-*co*-MMA-*b*-pS block copolymer brushes exhibited considerably different dispersion behavior. Particularly, colloids with $pSP_{0.2}$-*co*-$MMA_{0.8}$ films aggregated and sedimented out of toluene suspension following UV light irradiation, while pSP-*co*-MMA-*b*-pS treated particles remained well dispersed. The ability to synthesize block copolymer brushes by subsequent quenching and reinitiation confirms the "living" nature of the polymerization reactions examined here.

Photochromism of SiO_2-*g*-pSP-*co*-MMA Core−Shell Particles. The photochromic reaction of the spirobenzopyran moiety is depicted in Scheme 2. Upon UV irradiation, the neutral and colorless spirobenzopyran (SP) undergoes a ring-opening isomerization to form a zwitterionic blue/purple merocyanine (MC). The reverse process is facilitated by visible light or heat and will occur spontaneously at room temperature, albeit slower. These reactions are accompanied by characteristic changes in the UV/vis absorption spectra, which strongly depend on the polarity of the microenvironment surrounding the photochromic molecule.[30,52] Consequently, the presence of the polymer matrix and the solvent polarity are expected to significantly affect the SP photochromic behavior. Moreover, because of the high grafting density achievable with the ATRP approach,[44] the isomerization reactions within pSP-*co*-MMA polymeric brushes may be influenced by steric constraints.

Absorption spectra of 927 nm diameter SiO_2 colloids derivatized with pSP-*co*-MMA brushes and dispersed in THF or toluene are shown in Figure 4. Analogous absorption spectra have been acquired for monomeric SP and free $pSP_{0.2}$-*co*-$MMA_{0.8}$ polymers with the pertinent data summarized in Table 2.

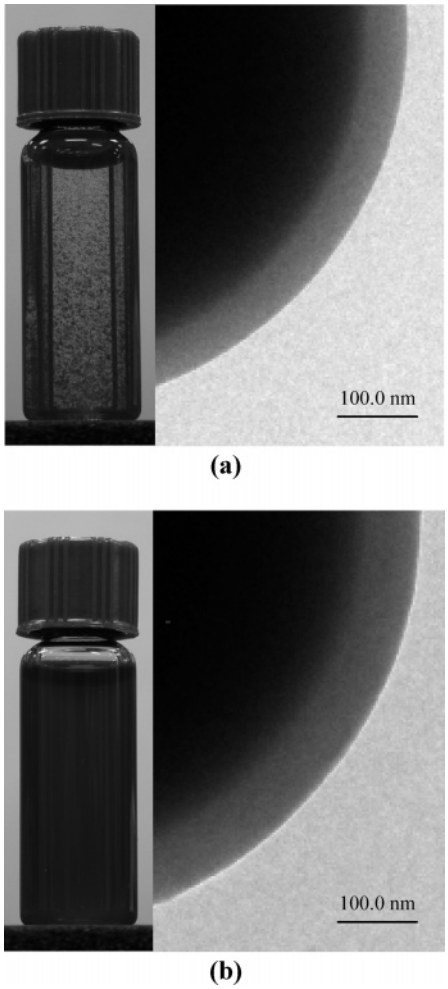

Figure 3. TEM micrographs showing the increase in the layer thickness following block copolymerization of styrene from SiO_2-*g*-$pSP_{0.2}$-*co*-$MMA_{0.8}$ core−shell particles. (a) The initial polymerization of $pSP_{0.2}$-*co*-$MMA_{0.8}$ brush (see Figure 2 caption for details) was quenched with excess $CuCl_2$ after 173 min, giving 56.3 ± 3.2 nm thick copolymer film. (b) Subsequent ATRP of styrene increased the layer thickness to 77.4 ± 4.5 nm. Polymerization conditions were as follows: [styrene] = 6.2 M, [CuBr] = 2.1×10^{-2} M; [$CuCl_2$] = 6.4×10^{-4} M; [PMDETA] = 7.9×10^{-2} M in anisole solvent with temperature = 95 °C and reaction time = 20 h. Insets in the figures show dispersion behavior in toluene following UV light excitation.

It is apparent from Figure 4 data that in addition to the absorption peak at $\lambda_{max} = 578-598$ nm there is a pronounced shoulder near $\lambda = 540-560$ nm. While the main peak can be ascribed to the open merocyanines in the trans form around the double bond,[18,53] the shoulder is most likely due to the formation of molecular H-stacks characterized by antiparallel alignment of alternate MC dipoles.[54−56] The development of J-stacks with parallel orientation of dipoles absorbing in $\lambda = 600-640$ nm range was not observed here.[56] The toluene spectrum is also characterized by a significant blue shift in λ_{max} relative to the THF data, which indicates a significantly more polar photochrome microenvironment. This is likely the result of a closer proximity of polar merocyanines in the polymeric brush under poor solvency conditions or by MC solvation by the more polar poly(methyl methacrylate) ester side groups.[18,57] Conversely, λ_{max} was red-shifted for the SP monomer in toluene by ~18 nm compared with the THF spectrum (see Table 2), emphasizing the importance of the polymer matrix in controlling the photochrome microenvironment.

First-order rate constants for the SP → MC coloration and MC → SP bleaching processes of SP monomers and $pSP_{0.2}$-

Table 2. Calculated Rate Constants for the SP → MC, and MC → SP Isomerization Reactions at 25 °C

species[a]/solvent	λ_{max}[b] (nm)	$(1-f)$[c]	k_c[d] (10^2 s^{-1})	k_d or k_{d1}[e] (s^{-1})	k_{d2}[e] (s^{-1})
monomer/THF	590.4 ± 1.0	0	29 ± 2	$(4.8 \pm 0.1) \times 10^{-2}$	
monomer/toluene	608.3 ± 0.8	0	29 ± 2	$(4.9 \pm 0.1) \times 10^{-2}$	
polymer/THF	586.6 ± 0.8	0	23 ± 7	$(1.4 \pm 0.1) \times 10^{-2}$	
polymer/toluene	582 ± 5	0	15 ± 2	$(1.9 \pm 0.2) \times 10^{-3}$	
particles/THF	598−590.5	0.50	15 ± 2	$(5.3 \pm 0.6) \times 10^{-3}$	$(4.3 \pm 0.5) \times 10^{-4}$
particles/toluene	585−578	0.17	8.3 ± 1.6	$(8.4 \pm 0.3) \times 10^{-4}$	$(6.3 \pm 2.8) \times 10^{-5}$

[a] Monomer = SP with [SP] = 4.6×10^{-6}−4.6×10^{-5} M; polymer = $pSP_{0.2}$-*co*-$MMA_{0.8}$ with [polymer] = 3.7×10^{-6}−3.7×10^{-5} g/mL; particles = 927 nm diameter SiO_2-*g*-$pSP_{0.2}$-*co*-$MMA_{0.8}$ with [particles] = 9.4×10^{-5}−3.5×10^{-4} g/mL. [b] Position of the visible absorption peak. When range is given, first number corresponds to spectrum immediately following UV irradiation, while the second represents data in the late stages of MC → SP conversion. [c] Fraction of the long-lived MC species (see eq 4). [d] First-order rate constant for the SP → MC "coloration" reaction determined from eq 3. Data combine measurements made at three different concentrations varying from 9.4×10^{-5} to 3.5×10^{-4} g/mL. Identical results were obtained at all three concentrations. [e] In the case of SP monomer and $pSP_{0.2}$-*co*-$MMA_{0.8}$ polymer the MC → SP isomerization kinetics were well described by a monoexponential decay (eq 3) with the rate constant denoted by k_d. For $pSP_{0.2}$-*co*-$MMA_{0.8}$ copolymer brushes grafted onto SiO_2 particles, eq 4 expressing superposition of two exponents fit the data accurately. Thus, k_{d1} represents rate constant for the shorter-lived MC species, while k_{d2} denotes the rate constant for the longer-lived analogue. Data combine measurements made at three different concentrations varying from 9.4×10^{-5} to 3.5×10^{-4} g/mL. Identical results were obtained at all three concentrations.

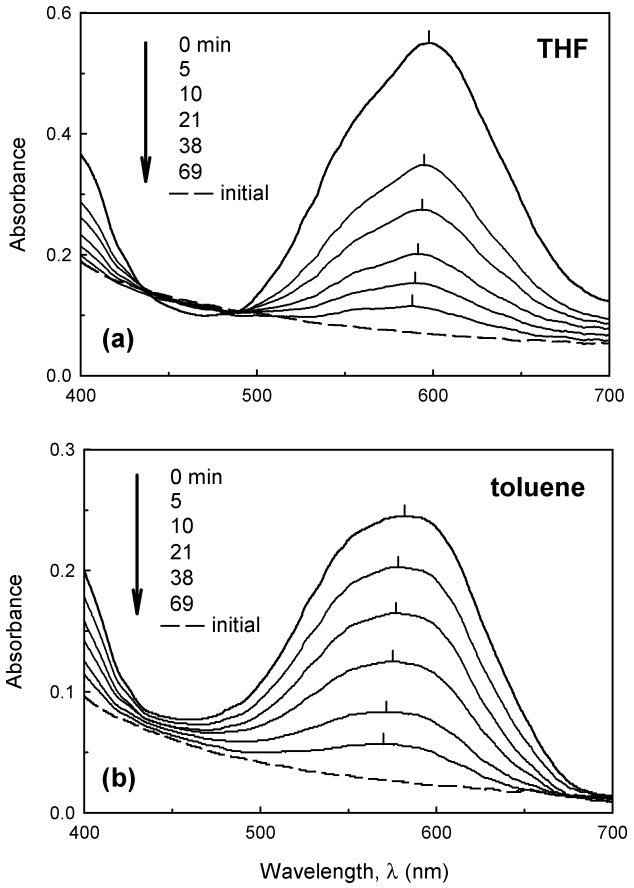

Figure 4. Changes in absorption spectra of 927 nm diameter SiO_2 colloids derivatized with $pSP_{0.2}$-*co*-$MMA_{0.8}$ copolymer brush and dispersed in (a) THF and (b) toluene. The sample concentration was 1.8×10^{-4} g/mL. The broken line represents data before UV irradiation; while solid lines correspond to spectra acquired after the UV treatment at the times indicated.

co-$MMA_{0.8}$ copolymers (see Table 2) were determined from the following equation.[52]

$$-\ln\left(\frac{A(t)-A_e}{A(0)-A_e}\right) = kt \qquad (3)$$

Here $A(t)$ and $A(0)$ denote the absorbance at λ_{max} at time t and at the beginning of the coloration or bleaching process. Similarly, A_e represents the absorbance at λ_{max} after reaching the photostationary state. Because the equilibrium constant for the MC ↔ SP isomerization reaction is no greater than 10^{-2}, k gives a direct measure of coloration or decoloration kinetics (i.e., back-reactions during coloration or bleaching processes are negligible).[52] Equation 3 has also been used to determine the coloration rate constant, k_c, for the SP → MC reaction in $pSP_{0.2}$-*co*-$MMA_{0.8}$ brushes on silica colloids. However, the bleaching process in that case was well fitted by a superposition of two first-order rate processes.[30]

$$\frac{A(t)-A_e}{A(0)-A_e} = f\exp(-k_{d1}t) + (1-f)\exp(-k_{d2}t) \qquad (4)$$

Here, f and $(1-f)$ denote fractions of MC moieties decaying faster with a rate constant k_{d1} and slower with k_{d2}, respectively. The slower decaying MC species were found to constitute H-stacks with a UV−vis absorption near $\lambda = 560$ nm, while the faster relaxation rate was attributed to individual, unassociated merocyanines.[54,55] Thus, the relaxation process in Figure 4 shows relative enrichment of the polymeric brush with longer-lived MC species on fading. Moreover, the MC → SP isomerization within copolymer brushes is characterized by higher fraction of slower decaying MC species in THF compared to toluene (see Table 2). This might be due to the fact that polymer brushes in THF are more solvated, allowing for chain reorganization and facilitating the formation of molecular MC aggregates. In toluene, after UV irradiation, polymer chains find themselves under poor solvency conditions. Therefore, brush penetration by solvent molecules is greatly limited, and chains are restricted from reorganizing to form MC complexes.

Decoloration data for 927 nm diameter SiO_2-*g*-$pSP_{0.2}$-*co*-$MMA_{0.8}$ core−shell particles dispersed in THF and toluene are illustrated in Figure 5 along with fits to eq 4. The corresponding k_{d1} and k_{d2} values were found to be order of magnitude lower in toluene (see Table 2). The fact that the bleaching process was found to be ~6−7 times faster in THF for both derivatized particles and free polymers points to the much better solvation of MC groups by that solvent and higher chain mobility. The same argument explains the approximately twice as fast SP → MC isomerization in THF. Almost equal k_c and k_d values for monomeric SP in both solvents further emphasize the importance of polymer−solvent interactions in controlling the photochromic process.

The kinetic data in Table 2 also illustrates the progressive slowing of both isomerization reactions following incorporation of the SP photochrome first into a polymer chain and then into a densely grafted polymeric brush. This is to be expected from increased steric confinement. However, if steric effects alone determined retardation, k_c and k_d should be similarly affected.

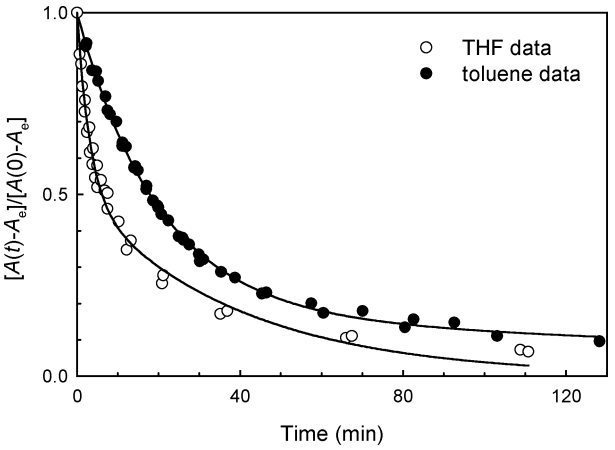

Figure 5. Kinetics of MC → SP bleaching process for 927 nm diameter SiO_2-*g*-$pSP_{0.2}$-*co*-$MMA_{0.8}$ core−shell particles dispersed in THF and toluene. Data combine the measurements at three different concentrations ranging from 9.4×10^{-5} to 3.5×10^{-4} g/mL. Solid lines represent best fits to eq 4.

Meanwhile, upon transition from a free SP molecule to the brush entrapped species k_c decreased by a factor of 2 in THF and by 3.4 in toluene. At the same time, k_d decreased by a factor of 9 and 60 for the corresponding solvents. This suggests stabilization of MC moieties via interaction with the surrounding polymer matrix, with the extent of such stabilization strongly mediated by the solvent properties.

It should also be noted that the rate constants determined here for the $pSP_{0.2}$-*co*-$MMA_{0.8}$ polymer bushes in toluene (i.e., $k_{d1} = 8.4 \times 10^{-4}$ s^{-1}, $k_{d2} = 6.3 \times 10^{-5}$ s^{-1}) are comparable with the dry film values. Specifically, Eckhardt et al. reported $k_{d1} = 8 \times 10^{-4}$ s^{-1} and $k_{d2} = 7 \times 10^{-5}$ s^{-1} for a copolymer film comprised of 1:1 isobutyl methacrylate and *n*-butyl methacrylate doped with 15% w/w SP.[56] Similar decoloration rate constants were obtained by Ueda et al. in the case of SP monolayers on silica particles dispersed in cyclohexane, CCl_4, and $CHCl_3$.[30] The authors found $k_{d1} = 5.2 \times 10^{-4}$−$7.3 \times 10^{-4}$ s^{-1} and $k_{d2} = 3.3 \times 10^{-5}$−$6.1 \times 10^{-5}$ s^{-1} for SP moiety attached to the silica surface by a seven-carbon chain. When a longer spacer was used (i.e., 15-carbon chain), these rate constants increased markedly. This comparison further supports a poor solvency condition for UV-irradiated $pSP_{0.2}$-*co*-$MMA_{0.8}$ polymer brushes in toluene, which behave like a solid matrix even when in contact with the solvent. The response changes considerably in THF where both bleaching processes are much faster, implying better solvent penetration of the brush.

Finally, significant property changes of SP containing polymers following application of light stimulus have been linked to significant changes in polymer conformation. In turn, these photoinduced conformational transformations were utilized to control contractile behavior,[17,58] solution viscosity,[19,57] and membrane permeability.[8,9] In a forthcoming publication we report on how the photostimulated conformational changes in pSP-*co*-MMA polymer bushes grafted onto silica particles and surfaces affect colloidal stability, particulate suspension viscosity, and particle deposition.[45,59]

Conclusions

Application of the ATRP methods to the synthesis of functional colloidal particles with a core−shell architecture confirmed the robustness and versatility of this living polymerization approach. Optimization of the reaction conditions allowed reproducible formation of grafted pSP-*co*-MMA copolymer brushes up to 80 nm thick with high grafting density. The type of surface-bound initiator and its concentration along with the choice of catalytic system markedly affected the final brush thickness. Polymerization kinetics indicated that termination reactions cause relatively low monomer conversions and film growth retardation. However, successful synthesis of block pSP-*co*-MMA-*b*-pS copolymer brushes by reaction quenching and subsequent reinitiation confirmed the "living" character of the polymerization. UV/vis spectral analysis of the pSP-*co*-MMA copolymer brushes following UV irradiation indicated the presence of free and H-stack associated merocyanines in both THF and toluene. This is supported by the kinetics of the bleaching process, which is described by the superposition of two first-order relaxation reactions corresponding to the two distinct MC species. At the same time, monomer and polymer kinetics followed first-order rate laws, indicating the absence of MC associations. Progressive slowing of both coloration and decoloration isomerization reactions following incorporation of the SP photochrome first into a polymer chain and then into a densely grafted polymeric brush points to significant steric crowding in pSP-*co*-MMA brushes. However, data also suggests stabilization of the MC moiety by the interaction with the surrounding polymer matrix. The extent of this stabilization is strongly mediated by the solvent properties. In fact, bleaching process are ∼6−7 times faster in THF for both the derivatized particles and free polymers, indicating much better solvation of MC groups and higher chain mobility in THF. Finally, UV irradiated $pSP_{0.2}$-*co*-$MMA_{0.8}$ polymer brushes in toluene were found to behave as solid, dry films with respect to MC → SP reaction kinetics and point to poor solvency conditions.

Acknowledgment. Sandia is a multiprogram laboratory operated by Sandia Corp., a Lockheed Martin Co., for the United States Department of Energy's National Nuclear Security Administration under Contract DE-AC04-94AL85000.

References and Notes

(1) Tazuke, S.; Kurihara, S.; Yamaguchi, H.; Ikeda, T. *J. Phys. Chem.* **1987**, *91*, 249−251.
(2) Katz, E.; Liondagan, M.; Willner, I. *J. Electroanal. Chem.* **1995**, *382*, 25−31.
(3) Rosario, R.; Gust, D.; Hayes, M.; Jahnke, F.; Springer, J.; Garcia, A. A. *Langmuir* **2002**, *18*, 8062−8069.
(4) Kinoshita, T. *J. Photochem. Photobiol. B* **1998**, *42*, 12−19.
(5) Oh, S.-K.; Nakagawa, M.; Ichimura, K. *J. Mater. Chem.* **2002**, *12*, 2262−2269.
(6) Tachibana, H.; Yamanaka, Y.; Matsumoto, M. *J. Mater. Chem.* **2002**, *12*, 938−942.
(7) Seki, T.; Fukuchi, T.; Ichimura, K. *Langmuir* **2002**, *18*, 5462−5467.
(8) Park, Y. S.; Ito, Y.; Imanishi, Y. *Macromolecules* **1998**, *31*, 2606−2610.
(9) Chung, D. J.; Ito, Y.; Imanishi, Y. *J. Appl. Polym. Sci.* **1994**, *51*, 2027−2033.
(10) Drummond, C. J.; Albers, S.; Furlong, D. N.; Wells, D. *Langmuir* **1991**, *7*, 2409−2411.
(11) Sheng, T.; Smith, K. A.; Hatton, T. A. *Langmuir* **2003**, *19*, 10764−10773.
(12) Kim, C. H.; Kim, D. K.; Lee, J. H.; Lee, K. S. *Mol. Cryst. Liq. Cryst.* **2001**, *370*, 131−134.
(13) Prasa, S. K.; Nair, G. G. *Adv. Mater.* **2001**, *13*, 40−43.
(14) Suzuki, Y.; Ozawa, K.; Hosoki, A.; Ichimura, K. *Polym. Bull.* **1987**, *17*, 285−291.
(15) Higuchi, A.; Hamamura, A.; Shindo, Y.; Kitamura, H.; Yoon, B. O.; Mori, T.; Uyama, T.; Umezawa, A. *Biomacromolecules* **2004**, *5*, 1770−1774.
(16) Kobayashi, N.; Sato, S.; Takazawa, K.; Ikeda, K.; Hirohashi, R. *Electrochim. Acta* **1995**, *40*, 2309−2311.
(17) Alonso, M.; Reboto, V.; Guiscardo, L.; San Martin, A.; Rodriguez-Cabello, J. C. *Macromolecules* **2000**, *33*, 9480−9482.
(18) Irie, M.; Iwayanagi, T.; Taniguchi, Y. *Macromolecules* **1985**, *18*, 2418−2422.
(19) Irie, M.; Hayashi, K.; Menju, A. *Polym. Photochem.* **1981**, *1*, 233−242.

(20) Kimura, K.; Nakamura, N.; Sakamoto, H.; Uda, R. M.; Sumida, M.; Yokoyama, M. *Bull. Chem. Soc. Jpn.* **2003**, *76*, 209−215.
(21) Seki, T.; Sekizawa, H.; Ichimura, K. *Polymer* **1997**, *38*, 725−728.
(22) Irie, M.; Suzuki, T. *Makromol Chem., Rapid Commun.* **1987**, *8*, 607−610.
(23) Irie, M.; Iga, R. *Makromol Chem., Rapid Commun.* **1985**, *6*, 403−405.
(24) Ishihara, K.; Hamada, N.; Kato, S.; Shinohara, I. *J. Polym. Sci., Polym. Chem.* **1984**, *22*, 121−128.
(25) Konak, C.; Kopeckova, P.; Kopecek, J. *J. Colloid Interface Sci.* **1994**, *168*, 235−241.
(26) Imai, Y.; Adachi, K.; Naka, K.; Chujo, Y. *Polym. Bull.* **2000**, *44*, 9−15.
(27) Quian, G.; Wang, M. *J. Chin. Ceram. Soc.* **2001**, *29*, 596−601.
(28) Ueda, M.; Kim, H. B.; Ichimura, K. *J. Mater. Chem.* **1994**, *4*, 883−889.
(29) Sugiyama, K.; Nakano, H.; Ohga, K. *Macromol. Chem. Phys.* **1994**, *195*, 3915−3928.
(30) Ueda, M.; Kudo, K.; Ichimura, K. *J. Mater. Chem.* **1995**, *5*, 1007−1011.
(31) Jia-Ling, P.; Hanna, J.; Kokado, H. *J. Imaging Sci.* **1989**, *32*, 232−237.
(32) Teranishi, T.; Yokoyama, M.; Sakamoto, H.; Kimura, K. *Mol. Cryst. Liq. Cryst.* **2000**, *344*, 271−276.
(33) Ruslim, C.; Ichimura, K. *Adv. Mater.* **2001**, *13*, 37−40.
(34) Murata, K.; Aoki, M.; Suzuki, T.; Harada, T.; Kawabata, H.; Komori, T.; Obseto, F.; Ueda, K.; Shinkai, S. *J. Am. Chem. Soc.* **1994**, *116*, 6664−6676.
(35) Ciampolini, M.; Nardi, N. *Inorg. Chem.* **1966**, *5*, 41−44.
(36) Matyjaszewski, K.; Miller, P. J.; Shukla, N.; Immaraporn, B.; Gelman, A.; Luokala, B. B.; Siclovan, T. M.; Kickelbick, G.; Vallant, T.; Hoffmann, H.; Pakula, T. *Macromolecules* **1999**, *32*, 8716−8724.
(37) Raymo, F. M.; Giordani, S. *J. Am. Chem. Soc.* **2001**, *123*, 4651−4652.
(38) Chung, D.-J.; Yoshihiro, I.; Imanishi, Y. *J. Appl. Polym. Sci.* **1994**, *51*, 2027−2033.
(39) Ziegler, M. J.; Matyjaszewski, K. *Macromolecules* **2001**, *34*, 415−424.
(40) Xia, J.; Matyjaszewski, K. *Macromolecules* **1997**, *30*, 7697−7700.
(41) Xiao, D.; Wirth, M. J., W. *Macromolecules* **2002**, *35*, 2919−2925.
(42) Ejaz, M.; Yamamoto, S.; Ohno, K.; Tsujii, Y.; Fukuda, T. *Macromolecules* **1998**, *31*, 5934.
(43) Ando, T.; Kamigaito, M.; Sawamoto, M. *Tetrahedron* **1997**, *53*, 15445−15457.
(44) Kamigaito, M.; Ando, T.; Sawamoto, M. *Chem. Rev.* **2001**, *101*, 3689−3745.
(45) Bell, N. S.; Piech, M. *Langmuir*, in press.
(46) Husseman, M.; Malmstroem, E. E.; McNamara, M.; Mate, M.; Mecerreyes, D.; Benoit, D. G.; Hedrick, J. L.; Mansky, P.; Huang, E.; Russell, T. P.; Hawker, C. J. *Macromolecules* **1999**, *32*, 1424−1431.
(47) Ejaz, M.; Tsujii, Y.; Fukuda, T. *Polymer* **2001**, *42*, 6811−6815.
(48) Savin, D. A.; Pyun, J.; Patterson, G. D.; Kowalewski, T. *J. Polym. Sci., Part B* **2002**, *40*, 2667−2676.
(49) Carrot, G.; Diamanti, S.; Manuszak, M.; Charleux, B.; Vairon, J.-P. *J. Polym. Sci., Part A* **2001**, *39*, 4294−4301.
(50) Pyun, J.; Jia, S.; Kowalewski, T.; Patterson, G. D.; Matyjaszewski, K. *Macromolecules* **2003**, *36*, 5094−5104.
(51) Kim, J. B.; Huang, W.; Bruening, M. L.; Baker, G. L. *Macromolecules* **2002**, *35*, 5410−5416.
(52) Flannery, J. B., Jr. *J. Am. Chem. Soc.* **1968**, *90*, 5660−5671.
(53) Kalisky, Y.; Williams, D. J. *Macromolecules* **1984**, *17*, 292−296.
(54) Goldburt, E.; Shvartsman, F.; Krongauz V. *Macromolecules* **1984**, *17*, 1225−1230.
(55) Goldburt, E.; Krongauz, V. *Macromolecules* **1986**, *19*, 246−247.
(56) Eckhardt, H.; Bose, A.; Krongauz, V. A. *Polymer* **1987**, *28*, 1959−1964.
(57) Irie, M.; Menju, A.; Hayashi, K. *Macromolecules* **1979**, *12*, 1176−1180.
(58) Smets, G.; Braeken, J.; Irie, M. *Pure Appl. Chem.* **1978**, *50*, 845−856.
(59) Piech, M.; George, M. C.; Bell, N. S.; Braun, P. V., *Langmuir*, in press.

MA0512760